Part III

Chapter 7

Optimized Linear Control

The paper proposes a novel control method for analog PMAs – *Multivariable Enhanced Cascade Control (MECC)*[1]. The topology has been devised to match the specific problems in general PMA systems. The primary motivation has been to meet any performance requirements even with very nonlinear and noisy plants. Recall that the fundamental control topologies analyzed in Chapter 6 were all bonded by inherent limitations, especially when attempting to realize high performance PMA systems. The proposed multiple-loop MECC topology overcomes several of these constraints, and enables flexible control of all essential system parameters by relatively simple means. MECC(N) and MECC(N,M) will be introduced as two general multiple-loop control methods. A general analysis of the properties will be presented. Following, the issue of robust MECC based PMA design is addressed by presenting optimized loop shaping methods. Case examples studies are investigated using the step-wise methodology for design and verification that was developed in Chapter 6.

7.1 Multivariable Enhanced Cascade Control (MECC)

MECC has two fundamental variants henceforth referred to as MECC(N) and MECC(M,N). A general block diagram for the N-loop MECC(N) topology is shown in Fig. 7.1, and Fig. 7.2 shows the extended general (N+M)-loop MECC(N,M) topology. Fundamentally, MECC is based on a recursive structure of N loops formed as an *enhanced*

[1] The MECC topologies and design methods are protected by a pending patent under the PCT arrangement (PCT/DK97/00497). The rights of the author and co-applicant (Bang & Olufsen A/S) shall be respected.

cascade from a single feedback source. MECC(N) is founded on feedback of v_p to one or several loops feeding into one or several pre-amplifier stages preceding the modulator and power switch. It may not seem obvious at first that MECC(N) should add any obvious advantages over VFC2. However, it will become apparent that this simple "extension" offers significant advantages with optimized compensator realization. MECC(N) is characterized by the following distinct points:

- A *single* feedback source.
- A *single* feedback path $A(s)$ independent upon the number of loops N, providing a minimal system complexity.
- The feedback path has a *low-pass* characteristic, to filter the noise from v_p *and* compensate the demodulation filter.
- An initializing $B_1(s)$ compensator block with special characteristics.
- A *recursive* structure with a set of preferably *identical* forward path compensator blocks $B_i(s)$.

Thus, the *Enhanced Cascade* refers to these special cascade control characteristics or this dedication of the cascade to the PMA control problem. Cascade control methods have previously been applied to linear power amplifier systems, in terms of e.g. the well-known Nested Differential Feedback Loop method (NDFL's) [Ch82]. This cascade structure has some resemblance with MECC(N) in that it uses only one feedback element with a differentiating characteristic. However, differentiating the HF- feedback source v_p in this case is clearly impossible, since it would cause the feedback compensator output to produce a severe amount of HF-output with amplitudes approaching infinity (!). Cherry's motivation for developing the NDFL control method was to realize improved control of the linear power amplification stage. The motivation for developing MECC for PMA system has been similar.

The MECC(N,M) topology shown in Fig. 7.2 is an extension in that an additional enhanced cascade is established from v_o to one or several chained pre-amplifier stages. MECC(N,M) encloses the PMA by two *connected* enhanced cascades, providing optimized control of all system parameters as distortion, noise, output impedance, PSRR etc. The connection between the enhanced cascades is established by the inherent compensation that is provided by unique A-block in the local enhance cascade. A fundamental constraint within MECC(N,M) system design is thus:

$$M \geq 1 \Rightarrow N \geq 1 \tag{7.1}$$

MECC(N) provides optimized control in dedicated applications where filter linearity is un-problematic and the load is known. The MECC(N,M) provides optimized control in all general applications. Both topologies have their place.

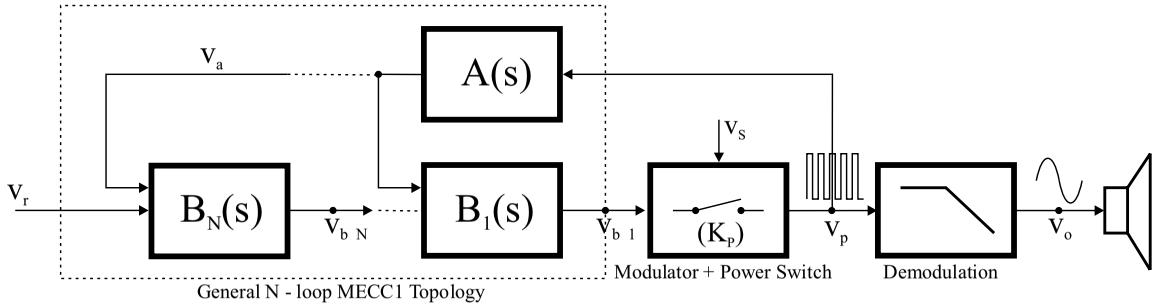

Fig. 7.1 General N-loop MECC(N) topology

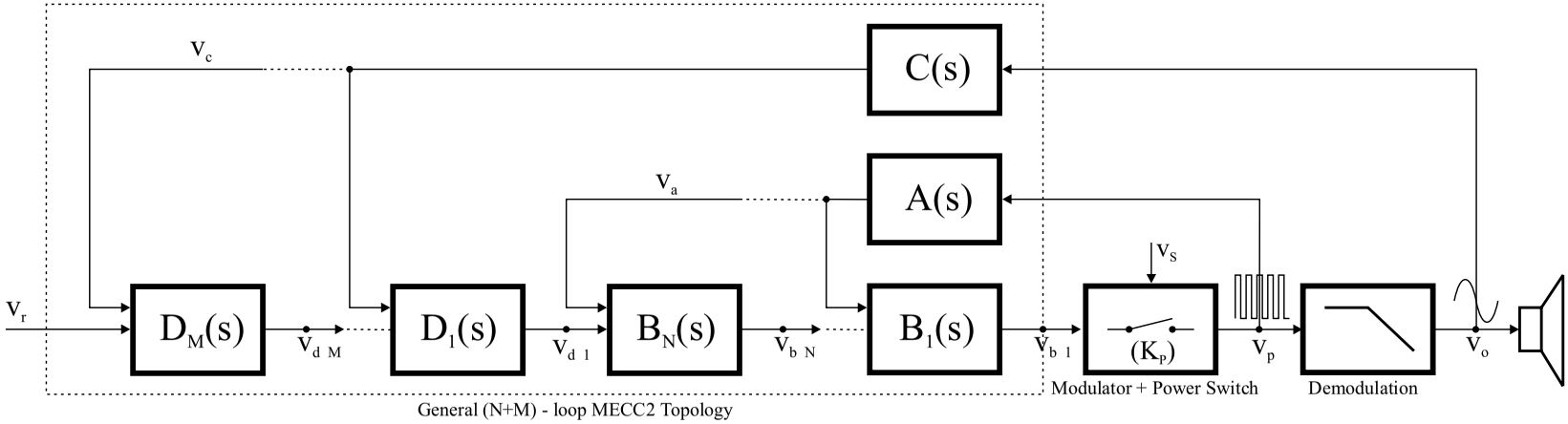

Fig. 7.2 General (N+M) - loop MECC(N,M) topology

7.1.1 Loop prototype based MECC(N) synthesis

In the following general N-loop MECC(N) controller synthesis is addressed, with the proposal of a general recursive design procedure. The foundation is a *loop prototype* based design approach that simplifies the synthesis, verification and implementation of the controller compared to individual parameter optimization of each loop in the multi-loop system. More important, prototype based design leads to a highly regular and flexible structure where the resulting performance is easily evaluated independent of the number of loops in the system. The flexibility arises from the loop number N that adds new flexibility to the loop shaping process in combination with the loop prototype specification. There are some fundamental prototypes with appealing characteristics. These prototypes and the prototype realization within the MECC(N) structure will be discussed in the following.

Leaky integrator Prototype

Consider the simple MECC(N) loop prototype specified:

$$L(s) = \frac{\tau_{i1}}{\tau_{uN}} \frac{1}{\tau_{i1} s + 1} \tag{7.2}$$

The "leaky integrator" characteristic of the loop prototype has the advantage of a constant gain within the frequency range determined by integrator time constant τ_{i1}. This can be used to implement a constant gain characteristic of the resulting sensitivity function within the target bandwidth, with a magnitude now determined exclusively by the loop number N. The bandwidth of the loop prototype is determined by τ_{uN}. The MECC(N) topology itself does not inherently provide an improved control of the PMA system, as the comparison with the topologically similar NDFL method clearly illustrated. A crucial aspect is the implementation of the loop prototype is the forward and feedback path compensators. The prototype is realized with the following A-compensator block characteristic:

$$A(s) = \frac{1}{K} \frac{1}{\tau_1 s + 1} \tag{7.3}$$

Where K determines the resulting closed loop gain within the target bandwidth of the system. The advantages of this A-block characteristic is the filtering of HF-noise from the v_p-generator in the case that carrier based modulation is used. Furthermore, the characteristic effectively prepares the local enhanced cascade for the application of a further global enhanced cascade by implementing a closed loop compensation effect. With $A(s)$ determined the following initial compensator B_1 will realize the desired loop prototype:

$$B_1(s) = \frac{K}{K_{PN}} \frac{\tau_{i1}}{\tau_1} \frac{\tau_1 s + 1}{\tau_{i1} s + 1} \tag{7.4}$$

K_{PN} is the nominal gain of the plant as defined in Chapter 6. Its axiomatic that the realization of $L(s)$ in each loop, combined with the unique feedback path compensator $A(s)$ results in a system transfer function that is independent of N, i.e. a closed loop prototype for the local enhanced cascade:

$$\begin{aligned} H_N(s) &= K\frac{L(s)}{1+L(s)} \\ &\approx K\frac{\tau_1 s+1}{\tau_{uN}s+1} \end{aligned} \tag{7.5}$$

The approximation will in general be very good with a reasonable selection of parameters. This will be described at a later point. The realization of $L(s)$ in all succeeding loops requires the following compensator characteristic:

$$B_i(s) = \frac{\tau_{i1}}{\tau_{uN}}\frac{\tau_{uN}s+1}{\tau_{i1}s+1} \tag{7.6}$$

With the loop prototype based approach, MECC(N) optimization only requires optimization of a few fundamental parameters, independent upon the number of loops N. Furthermore, each compensator is simple and straightforward to implement. Both issues are pleasant features.

Modified Leaky Integrator prototype
An obvious extension is to modify the leaky integrator characteristic to a second order characteristic:

$$L(s) = \frac{\tau_{i1}}{\tau_{uN}}\frac{1}{\tau_{i1}s+1}\frac{1}{\tau_2 s+1} \tag{7.7}$$

Realized by modifying the A-compensator to:

$$A(s) = \frac{1}{K}\frac{1}{\tau_1 s+1}\frac{1}{\tau_2 s+1} \tag{7.8}$$

The additional pole improves the demodulation in the local feedback path and lowers the bandwidth to carrier frequency ratio.

7.1.2 MECC(N) properties

The analysis of MECC(N) now proceeds with a more fundamental investigation of the system properties, based on the loop prototype and compensator characteristics. General expressions are derived for the effective sensitivity function and the resulting closed loop transfer function. First the simplified case where $N=2$ is considered. From Fig. 7.1 we get by simple algebraic manipulations:

$$v_o = K_{PN}B_1(B_2(v_r - Av_p) - Av_p) = K_{PN}B_1B_2\ v_r - K_{PN}(B_1B_2 + B_1)Av_p \tag{7.9}$$

Hence:

$$H_N = \frac{K_{PN} B_1 B_2}{1 + K_{PN} A(B_1 B_2 + B_1)} \qquad (N = 2) \tag{7.10}$$

Generalized to the general N-loop case we have from Fig. 7.1:

$$v_p = K_{PN} B_1 (B_2 (B_3 (\cdots B_N (v_r - A v_p) \cdots - A v_p) - A v_p) - A v_p) \tag{7.11}$$

This leads to the closed loop expression:

$$H_N = \frac{K_{PN} \prod_{i=1}^{N} B_i}{1 + K_{PN} A \left[\prod_{i=1}^{N} B_i + \prod_{i=1}^{N-1} B_i + \prod_{i=1}^{N-2} B_i + \cdots + B_2 B_1 + B_1 \right]} \tag{7.12}$$

Which reduces to the following compact expression:

$$H_N = \frac{K_{PN} \prod_{i=1}^{N} B_i}{1 + K_{PN} A \sum_{j=0}^{N-1} \left[\prod_{i=1}^{N-j} B_i \right]} \tag{7.13}$$

With the proposed leaky integrator prototype realized in each loop, it can be shown that H_N realizes the approximate expression as defined in (7.5). The significant importance of (7.13) becomes evident when investigating the effective system that is implemented by the MECC(N) topology. The *effective loop transfer function* L_N and – equivalently – the *effective sensitivity function* S_N are defined as:

$$L_N = K_{PN} A \sum_{j=0}^{N-1} \left[\prod_{i=1}^{N-j} B_i \right] \tag{7.14}$$

$$S_N = \frac{1}{1 + K_{PN} A \sum_{j=0}^{N-1} \left[\prod_{i=1}^{N-j} B_i \right]} \tag{7.15}$$

These parameters will be used to gain insight in the performance and robustness of the effective system that is realized by the MECC(N) topology. Consider a typical case where $|B_i| >> 1$ within the target frequency band. S_N is simplified to:

$$S_N \approx \frac{1}{K_{PN} A \prod_{i=1}^{N} B_i} \quad \forall \omega \quad \textit{within target frequency band} \tag{7.16}$$

This approximate relation shows that the effective sensitivity within the target frequency band is the product of the contributions of each individual loop. Subsequently, the performance can be controlled simply by the number of loops N. Every loop individually exhibits excellent stability, so adding or removing (identical) compensator blocks does not influence stability. Another important aspect is the *successive* improvement afforded by the enhanced cascade configuration as opposed to a single high bandwidth, high gain approach. The successive approach proves more efficient than a one-loop realization.

Control signal characteristics
Another important aspect is the control signal level throughout the system, in terms of the response of the individual compensator blocks to the reference input. The control signal transfer functions are easily derived:

$$H_{Bi,N} = \frac{v_{bi}}{v_r} = \frac{v_p}{v_r}\left(\frac{v_p}{v_{bi}}\right)^{-1} = \frac{H_N}{H_i} \approx 1 \tag{7.17}$$

$$H_{A,N} = \frac{v_a}{v_r} \approx 1 \tag{7.18}$$

The balanced control signals are another advantage gained by the loop prototype based design. The unity gain control signal transfer functions minimizes the requirements for e.g. dynamic range and linearity of the compensator components. Systems with non-balanced control signal may be limited by the compensator performance. A typical example of a system with non-balanced control signals is a single loop higher order control system with multiple series connected compensators.

7.1.3 MECC(N) loop shaping

In general, the process of MECC system design covers the same fundamental steps as for other linear control systems. The actual parameter optimization involving the specification of loop prototype and selection of the fundamental parameters is addressed in the

Parameter	Value	Comment
$f_1 = \frac{1}{2\pi\tau_{p1}}$	f_o	A-block parameter
$f_{i1} = \frac{1}{2\pi\tau_{i1}}$	$\frac{1}{10} f_{uN}$	Pole frequency for loop prototype $L(s)$
N	$N \leq 4$	Limit on necessary (and practical) number of loops in the MECC(N) structure
$f_2 = \frac{1}{2\pi\tau_2}$	20	Parameter for modified leaky integrator prototype
f_o	2	Demodulation filter natural frequency
Q_{oN}	$\frac{1}{\sqrt{3}}$	Demodulation filter Q (Bessel)
f_r	4	Reference filter natural frequency
Q_r	$\frac{1}{\sqrt{3}}$	Reference filter Q (Bessel).

Table 7.1 Proposed general MECC(N) parameter values.

following. Table 7.1 proposes a general set of parameters that serve as guideline to optimized MECC(N) design. The free parameters are the number of loops *N* and the loop prototype bandwidth f_{uN}. It should be emphasized that the parameters are optimized for the MECC(N) topology specifically, i.e. the parameters change if the system is extended to MECC(N,M). The fundamental parameter τ_{i1} is chosen to realize the desired characteristic of the loop prototype. The A-block parameter τ_1 is optimized to compensate the demodulation filter best possible and to demodulate the power stage output.

The tradeoffs between bandwidth, number of loops and loop prototype will be become clearer throughout the more detailed investigations of an illustrative case example.

7.1.4 MECC(N) case example

MECC(N) system synthesis is illustrated by a case example, using the general controller synthesis and verification steps in coherence with the methodology that was used throughout Chapter 6. A parametric analysis is performed where *N* is a variable parameter.

STEP 1: Specification

A case example system is considered for the full audio bandwidth with a desired system gain of $K = 26dB$. The equivalent power stage gain is assumed $K_{PN} = 26dB$. No specific performance criteria for the target frequency band are specified. Instead, a parametric analysis of the achievable performance vs. *N* is carried out.

STEP 2: Synthesis

The simple leaky integrator has been chosen as loop prototype. The prototype bandwidth is selected to $f_{uN} = 5$. The proposed parameters in Table 7.1 are used, and all sub-controllers in the MECC(N) structure are now defined.

STEP 3: Verification

Fig. 7.3 shows the components of first loop and the realization of the loop prototype $L(s)$. Following loops in the enhanced cascade are realized by the addition of further B_i blocks is shown in Fig. 7.4. Fig. 7.5 and Fig. 7.6 illustrate the effective loop transfer function L_N and sensitivity function S_N with the specified parameters. The Nth order transition caused by N poles and N-1 zeros in effective loop transfer is very pronounced from the parametric analysis in Fig. 7.5. The parametric investigation of the effective sensitivity function S_N verifies the excellent stability characteristics for the MECC(N) topology:

$$\left\| S_N \right\|_\infty < 1 \quad \forall \omega, N \tag{7.19}$$

This is a general property of MECC(N) with the proposed parameter values in Table 7.1. With the given loop prototype bandwidth we have:

$$S_M = -13 \cdot N \ (dB) \tag{7.20}$$

The system response is shown in Fig. 7.7. The response is dominated by the post filter. With the specified parameters, the resulting system frequency response is acceptable in the nominal load. Clearly, an improved frequency response and reduced sensitivity to load perturbations can be realized by increasing f_0. All essential specifications for the synthesized MECC(N) system are summarized in Table 7.2.

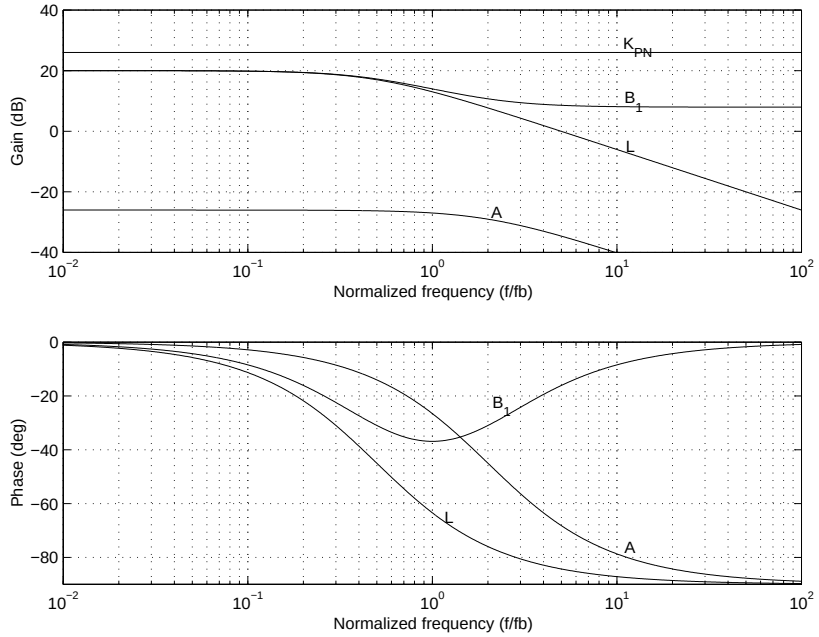

Fig. 7.3 MECC(N) Case example. Components of the first loop and resulting loop prototype $L(s)$.

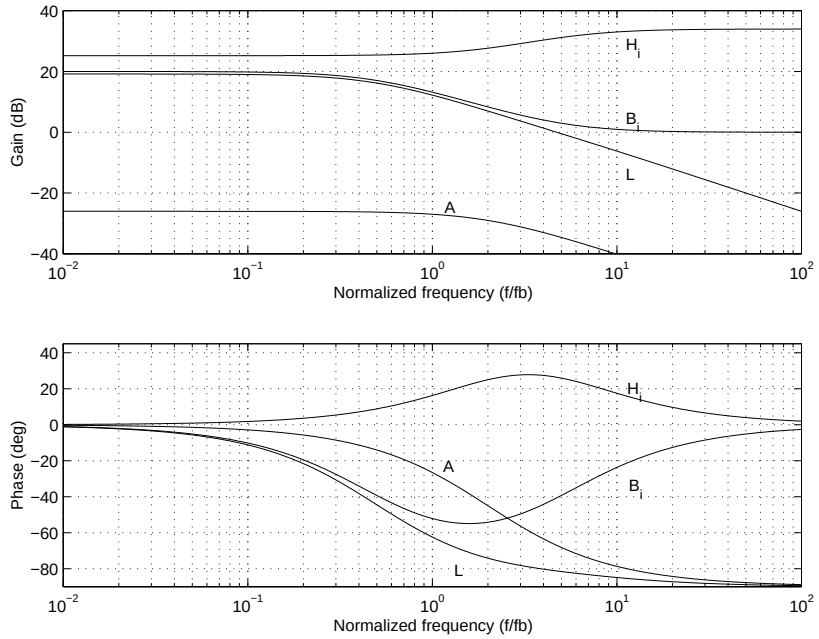

Fig. 7.4 MECC(N) case example. Components of any successive loop.

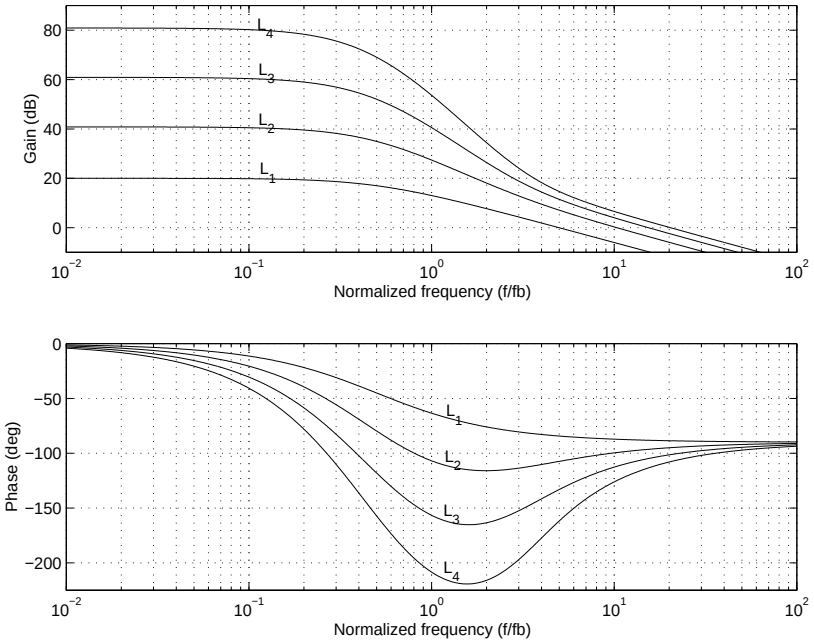

Fig. 7.5 MECC(N) parametric analysis of effective loop transfer function L_N . (*N = 1,2,3,4*).

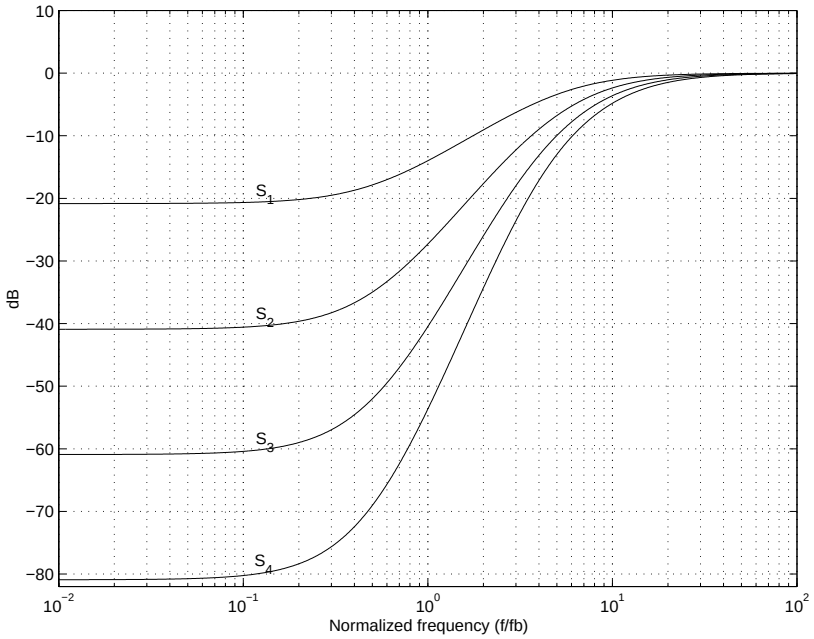

Fig. 7.6 MECC(N) parametric analysis of effective sensitivity function S_N . (*N = 1,2,3,4*).

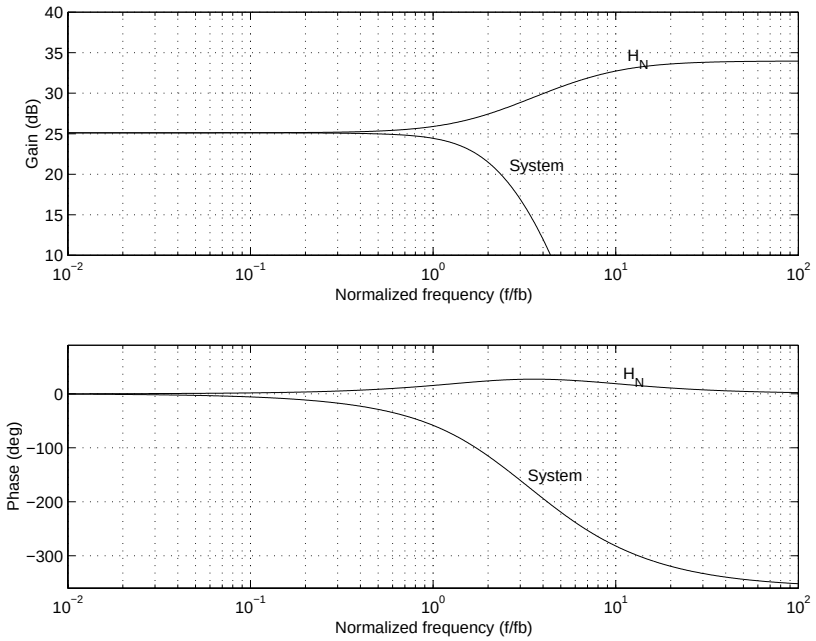

Fig. 7.7 MECC(N) case example system transfer function (independent of N).

Specification	Value	Comments
System gain	*25.1 dB*	20dB feedback.
Bandwidth	2	-3dB normalized system bandwidth.
Frequency response	$\pm 0.5dB$	Nominal system.
Phase response	$\pm 60^0$	Nominal system.
S_M	$-13 \cdot N\ dB$	Nominal system
$\|S_N\|_\infty$	$<1 \quad \forall \omega, N$	Peak of effective sensitivity function.

Table 7.2 Essential stability and performance of the synthesized general MECC(N) system

Modified Leaky Integrator Prototype

The realization of the proposed second order loop prototype is considered:

$$L_N(s) = \frac{\tau_{i1}}{\tau_{uN}} \frac{1}{\tau_{i1} s + 1} \frac{1}{\tau_2 s + 1} \tag{7.21}$$

The additional pole has the positive effect of improving the demodulation within the feedback path for all carrier based modulation methods and furthermore minimizes the effects of any non-modeled dynamics at higher frequencies. The bonding of the new parameter τ_2 to τ_{uN} (see Table 7.1) prevents any new degrees of freedom that would complicate the otherwise simple controller synthesis. Fig. 7.8 shows a parametric analysis of S_N for ($N = 1,2,3,4$). In terms of performance characteristics within the target frequency band, the differences are insignificant. The significant differences lies in the stability characteristics, i.e. $\|S_N\|_\infty$. Recall that $\|S_N\|_\infty < 1 \quad \forall \omega, N$ with the first order prototype whereas the following is realized with the second order loop prototype:

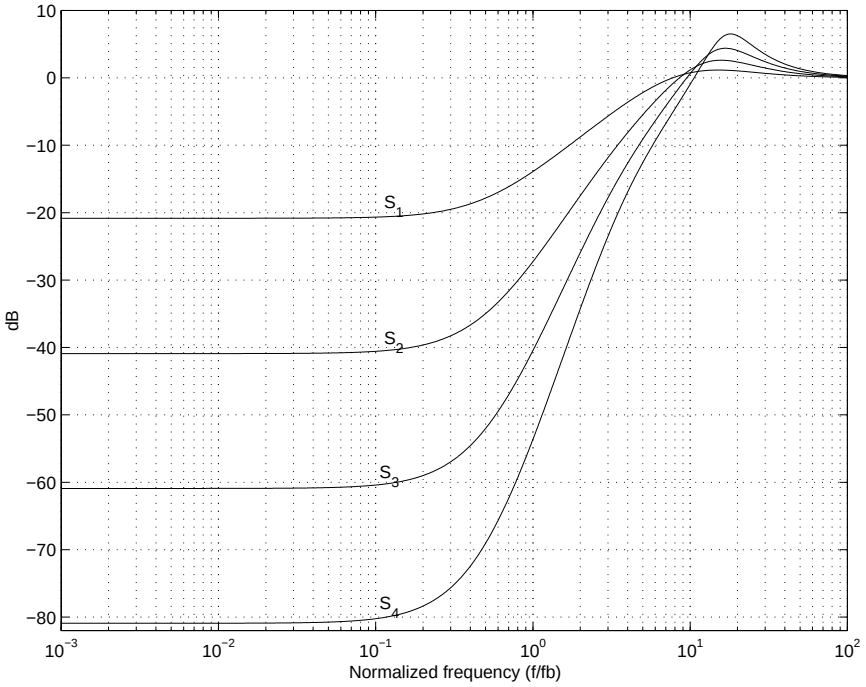

Fig. 7.8 S_N with the modified second order loop prototype. (*N = 1,2,3,4*)

N	1	2	3	4
$\|S_N\|_\infty$	1.13	1.35	1.65	2.11

Correspondingly, the second order prototype based design is accompanied by compromises on performance, i.e. *NP* requires *N*<3. Clearly, the second order prototype based system converges towards instability with N. It is possible to optimize each individual compensator in the MECC(N) structure to minimize this effect but the result is hardly as elegant and general as the simple recursive design. Instead, τ_2 should be modified if a higher order system is desired with the second order loop prototype.

STEP4: Robustness properties

With the given first order prototype based design there is no theoretical limit to the number of loops that can be implemented in the MECC(N) structure. In practice however, there will be restrictions on the number of loops in the local enhanced cascade arising from uncertainty on K_P and t_p. Due to the local feedback source, only perturbations on these parameters within the fundamental PMA are of concern. The important effects of K_P and t_p uncertainty are investigated by considering the following set of perturbed loop transfer functions:

$$L_{N,p}(r_K, t_p) = r_K K_{PN} A \sum_{j=0}^{N-1} \left[\prod_{i=1}^{N-j} B_{i,p} \right] \cdot e^{-t_p s} \qquad (7.22)$$

$$= r_K e^{-t_p s} L_N$$

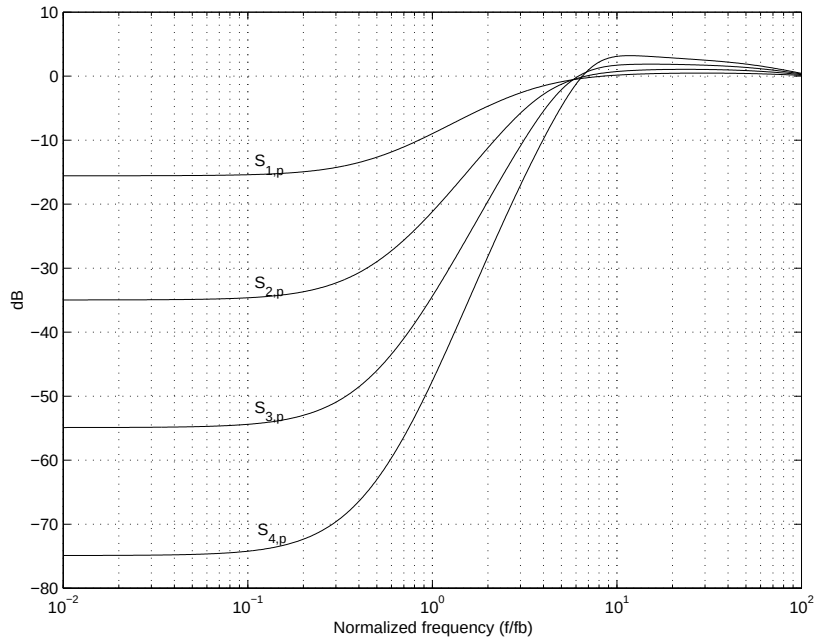

Fig. 7.9 Perturbed sensitivity functions $S_{N,p}(0.5,200ns)$ for the MECC(N) case example.

The isolation of the uncertain parameters from the sum in (7.22) makes the effects of perturbations easy to predict. This *visibility* of both types of perturbations should be credited to the regular expandable MECC(N) structure. Generally, it is difficult to directly predict the effects of perturbations in multi-loop systems. A parametric investigation of the robustness of the specific case is shown by the effective sensitivity is shown in Fig. 7.9. Only the worst-case plant is considered where $r_K = 0.5$ and $t_p = 200ns$. $\left\|S_{N,p}\right\|_\infty$ is determined in the four cases from Fig. 7.9:

N	1	2	3	4
$\left\|S_{N,p}\right\|_\infty$	1.05	1.13	1.24	1.44

Clearly, the topology is remarkable stable toward any perturbation within the *US*. *RS* and *RP* are satisfied. Specifically, it is worth noticing that the stability properties are nearly insensitive towards perturbations on K_P. Only performance is compromised in the *first* loop as shown in Fig. 7.9. This is a very pleasant characteristic of a higher order control system as MECC(N). Uncertainty on any parameter within the filter (e.g. on Q_o) will have the same influence on system performance as for the VFC2 system. Stability and robustness are not affected, but the frequency response of the total system is compromised since the filter is not controlled.

The parametric uncertainty within the compensator blocks is a concern in higher order control systems. The most important type is uncertainty on the compensator zeros which can be expressed as:

$$B_{i,p}(s) = \frac{\tau_{i1}}{\tau_{uN}} \frac{\alpha\tau_{uN}s+1}{\tau_{i1}s+1} \qquad \alpha_{\min} \le \alpha \le \alpha_{\min} \tag{7.23}$$

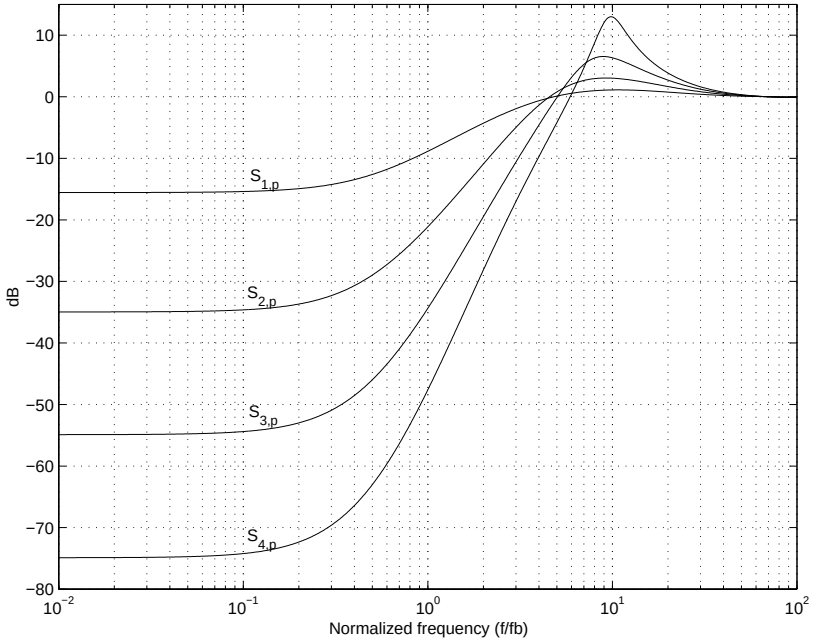

Fig. 7.10 Robustness investigations of MECC(N) with the proposed second order loop prototype.

The compensator poles will affect the target band performance but only marginally influence the stability characteristics that are determined by the characteristics well beyond the target frequency band. Investigations have shown that even 10% tolerance on the compensator zeros will only marginally influence stability and performance. To conclude, the MECC(N) system is a very robust higher order control system.

The robustness of MECC(N) based on the second order loop prototype is investigated in Fig. 7.10 by the perturbed sensitivity functions corresponding to the worst case parameter set within the Uncertainty Set. The following maximal peaks are determined:

N	1	2	3	4
$\left\|S_{N,p}\right\|_\infty$	1.13	1.42	2.12	4.47

Robust performance requires $N < 4$ in this worst-case situation. The second order design approach is as such a viable alternative to the first order loop prototype.

STEP5: Non-linear simulation

The case example is simulated with the non-linear 200W power stage that has been used throughout the investigations in Chapter 6. The investigations will focus on a illustrative triple loop case example, with sufficient compensation effect to honor even the most demanding investigations with a $S_M \approx -40$dB. The noisy NADD modulation method is chosen to illustrate the influence of carrier components on the controller signals. The carrier frequency selection is again based on SRI considerations. With $f_c = 500KHz$, the first order prototype design will potentially unstable due to SRI since $|L_3(j\omega_c)| \approx -6dB$ (see Fig. 7.5), whereas the second order loop prototype will have a sufficient margin to SRI since $|L_3(j\omega_c)| \approx -9dB$. The parameters for the non-linear investigation of MECC(3) are summarized below:

Parameter	Value
V_S	50V
V_T	2.5V
f_b	20KHz
f_c	500KHz
N	3
S_M	-40dB
$\|S_{N,p}\|_\infty$	2.12

Fig. 7.11 and Fig. 7.12 shows a functional simulation of the MECC(3) based PMAs with both first and second order loop prototypes. The system operates as desired with the specified gain with both prototypes. The compensator signals v_{b1}, v_{b2} and v_{b3} are *balanced* as determined in (7.17) and (7.18), and the simulation thus verifies this pleasant characteristic of MECC(N). The significant residual from the power stage superposed on v_{b1} is as predicted. The system is clearly on the edge of Slew Rate Instability, and the system is potentially unreliable since e.g. gain perturbation will lead to SRI. With the second order loop prototype, the HF content on all controller signals are reduced significantly as shown in the simulation in Fig. 7.12. The simulation documents the general advantages of the second order loop prototype.

Correction of General Non-linearity

The general correction effect offered by the MECC(N) system is investigated with non-linear model of the power stage in the form:

$$v_P(M) = K_{PN}(1 + c_1 M + c_2 M^2 + c_3 M^3) v_{b1} \tag{7.24}$$

This model has no direct relation with the actual non-linear PMA power stage, but exclusively serves to provide simple means form a *parametric* investigation of the error correction performed by the MECC(N) systems. Fig. 7.13 clearly verifies the successive improvement in performance with *N*. With quadruple loop control system applied to the non-linear model the improvement is 57dB or a reduction from 3.3% open loop THD to only 0.0044% THD with MECC(4). This verifies the successive correction effect of the multiple-loop system. Fig. 7.14 shows the compensator signals at M=0.9 for MECC(4). All controller outputs have the same magnitude as expected from (7.17) and (7.18).

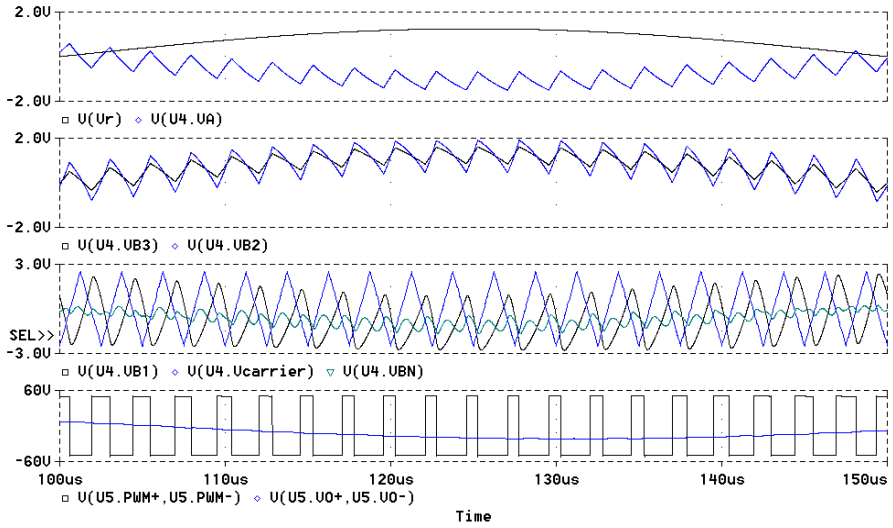

Fig. 7.11 Functional simulation of MECC(3) based on *first order loop prototype*. With $f_c = 500KHz$ the system operates on the edge of SRI. Top - Reference v_r and feedback v_a, Upper Mid - Forward compensator signals v_{b3} and v_{b2}, Lower mid – carrier and compensated output v_{b1} that is input to the modulator. The modulator input is also shown with the fundamental carrier removed by a tuned circuit. Bottom - power outputs v_p and v_o.

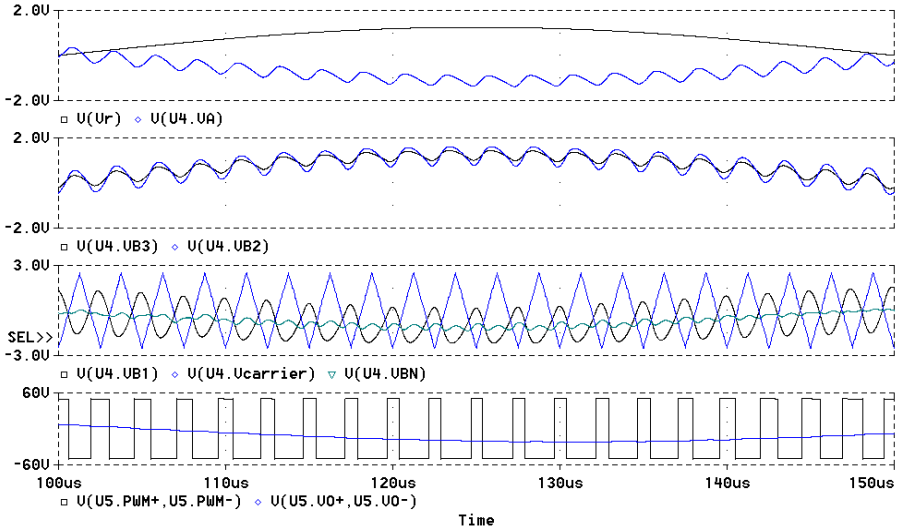

Fig. 7.12 Functional simulation of MECC(3) PMA system based on *2nd order loop prototype*. Top - Reference v_r and feedback v_a, Upper Mid - Forward compensator signals v_{b3} and v_{b2}, Lower mid – carrier and compensated output v_{b1} driving the modulator. Bottom - power outputs v_p and v_o.

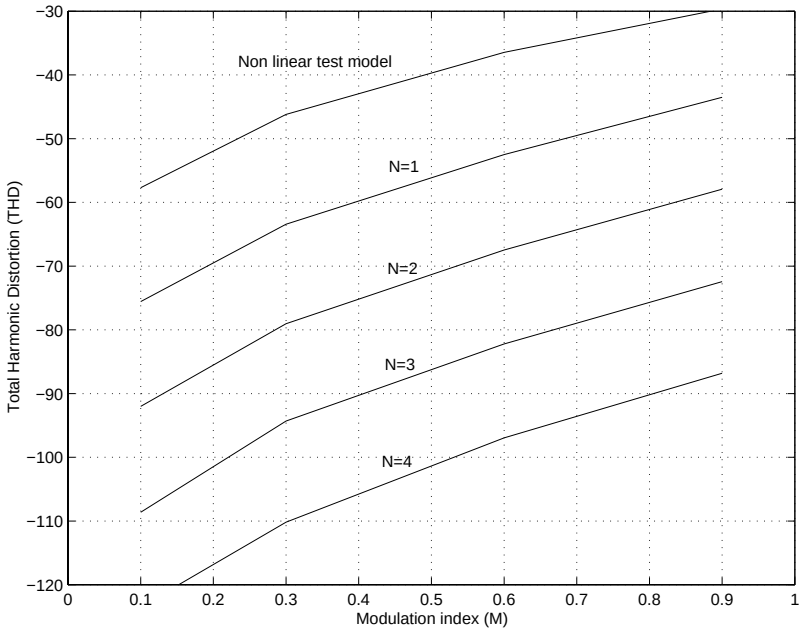

Fig. 7.13 THD vs. M with MECC(N) applied the non-linear plant. The signal frequency is 5KHz.

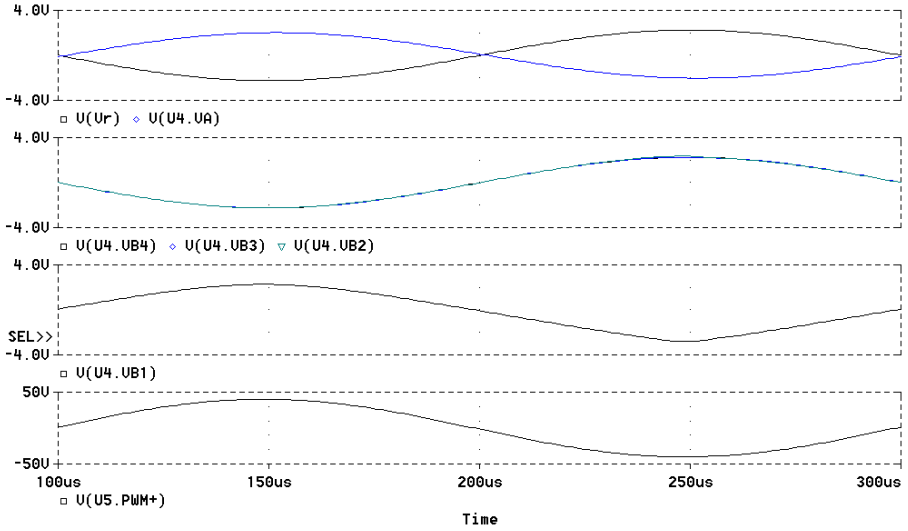

Fig. 7.14 THD vs. M with MECC(N) applied the non-linear plant. The signal frequency is 5KHz and M=0.9. Top - Reference v_r and feedback v_a, Upper Mid - Forward compensator signals v_{b4}, v_{b3} and v_{b2} (nearly identical), Lower mid – carrier and compensated output v_{b1} driving the modulator, Bottom - power outputs v_p and v_o. Note, that all control signals have equal magnitudes.

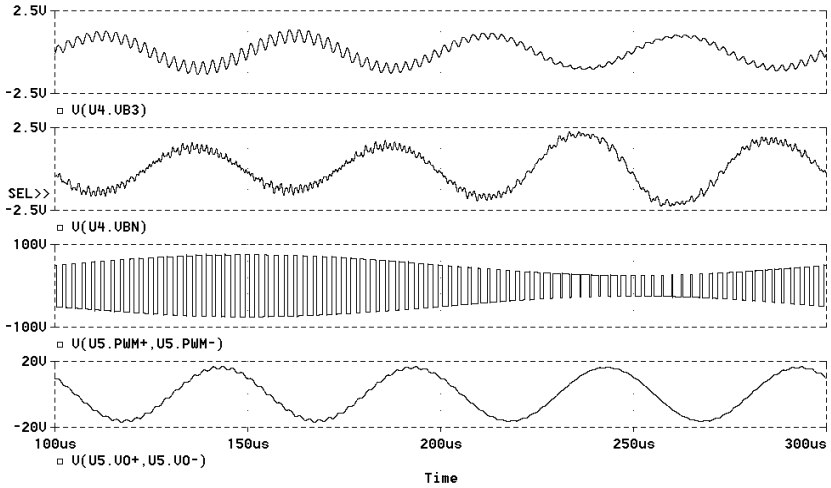

Fig. 7.15 Simulation of PAE error correction with MECC(3) system. Top – B_3 compensator output v_{b3}, Upper mid – B_1 compensator output v_{b1} with the carrier fundamental notched out. Lower mid and bottom shows the power stage outputs. The IM-distortion is effectively eliminated by a PSRR of 40dB at 20KHz.

PTE and PAE Correction

A simulation of PTE effects with a 5KHz signal frequency will verify a reduction in THD of about 40dB with the triple loop MECC(N) based controller, as theory would predict ($S_M \approx -40dB$). In terms of PAE error correction, the triple system has been simulated with a significant 50Vpp/5KHz perturbation superposed on V_S as show in Fig. 7.15. The intermodulation distortion is essentially eliminated by a PSRR of 40dB at 20KHz.

7.2 MECC(N,M)

The focus now turns to the extended topology with N local and M global loop formed in two linked enhanced cascades. The topology is founded on a MECC(N) design and should be seen as a direct extension of this topology. The MECC(N,M) topology is characterized by:

- A MECC(N) system, that is optimized specifically for the global enhanced cascade.
- A *single* feedback source v_o.
- A *single* feedback path compensator C.
- A D_1 compensator to initialize the cascade.
- A *recursive* structure with a set of preferably *identical* compensator blocks D_i.

The topological resemblance between MECC(N) and MECC(N,M) also leads to similarities in the synthesis of the to cascade structures. However, MECC(N,M) is constituted of two closely connected enhanced cascades, where the global enhanced cascade relies on the compensation from the local cascade. The following section will address all aspects MECC(N,M) design.

7.2.1 Loop prototype based MECC(N,M) synthesis

The control plant for the global enhance cascade is the MECC(N) controlled system $H_N(s)$ in series with the demodulation filter $F(s)$, which is assumed to be a standard second order characteristic:

$$H_N(s) \cong K\frac{\tau_1 s+1}{\tau_{uN} s+1} \tag{7.25}$$

$$F(s) = \frac{\omega_o^2}{s^2 + \frac{\omega_o}{Q_{oN}} s + \omega_o^2} \tag{7.26}$$

MECC(N,M) synthesis will be based on the specification of a unique loop prototype consistent with the approach for MECC(N) synthesis. A desirable loop prototype is again a leaky integrator characteristic:

$$L(s) = \frac{\tau_{i2}}{\tau_{uM}}\frac{1}{\tau_{i2} s+1} \tag{7.27}$$

Clearly, the unity gain frequency (bandwidth) of the loop prototype is determined by τ_{uM}. The requirement for a system gain K locks the compensator characteristic of the feedback path:

$$C(s) = \frac{1}{K} \tag{7.28}$$

No specific filtering is needed in C since the feedback source is demodulated. A connection between the local system and the global system is established by the following parameter assignments:

$$\tau_1 = \frac{1}{\omega_0} \quad \text{and} \quad f_{uN} > f_{uM} \tag{7.29}$$

This specific parameter assignment causes $H_N(s)F(s)$ to have a first order characteristic within the bandwidth of the of the local loop prototype for MECC(N). The initial compensator D_1 that will realize the global loop prototype can now be specified:

$$D_1(s) = \frac{\tau_{i2}}{\tau_{uM}} \frac{\tau_1 s + 1}{\tau_{i2} s + 1} \tag{7.30}$$

Assuming that $f_{uN} >> f_{uM}$, the general MECC(N,M) system response will be:

$$H_{N,M}(s) \approx K \frac{1}{\tau_{uM} s + 1} \tag{7.31}$$

$H_{N,M}$ should be considered as a closed loop prototype that is synthesized independent of M. This is axiomatic with a unique loop prototype and a unique feedback path. The general D_i - compensator that will realize the loop prototype in any succeeding loops is:

$$D_i(s) = \frac{\tau_{i2}}{\tau_{uM}} \frac{\tau_{uM} s + 1}{\tau_{i2} s + 1} \tag{7.32}$$

7.2.2 MECC(N,M) properties

Since the structure of both the local and global enhanced cascade is the same, many of the pleasant properties for MECC(N) can be generalized to MECC(N,M) directly. Fig. 7.2 yields the following relation:

$$v_o = H_N F D_1 (D_2 (D_3 (\cdots D_M (v_r - C v_o) \cdots - C v_o) - C v_o) - C v_o) \tag{7.33}$$

Or equivalently:

$$H_{N,M} = \frac{H_N F \prod_{i=1}^{M} D_i}{1 + H_N C F \sum_{j=0}^{M-1} \left[\prod_{i=1}^{M-j} D_i \right]} \tag{7.34}$$

The (N,M)-subscript in $H_{N,M}$ refers to that the M-loop MECC(N,M) design is based on the general N-loop MECC(N) system. The effective loop transfer function $L_{N,M}$ for the MECC(N,M) system is defined as:

$$L_{N,M} = H_N C F \sum_{j=0}^{M-1} \left[\prod_{i=1}^{M-j} D_i \right] \tag{7.35}$$

And the effective sensitivity function $S_{N,M}$ for MECC(N,M) equivalently:

$$S_{N,M} = \frac{1}{1 + H_N C \sum_{j=0}^{M-1} \left[\prod_{i=1}^{M-j} D_i \right]} \tag{7.36}$$

Within the target frequency band $S_{N,M}$ can be approximated by:

$$S_{N,M} \approx \frac{1}{1 + H_N C \prod_{i=1}^{M} D_i} \quad \forall \omega \text{ within target frequency band} \tag{7.37}$$

Looking at the resulting sensitivity function that specifies the reduced sensitivity to any errors within the fundamental elements of the PMA it is straightforward to show that the resulting sensitivity function is simply $S = S_N \cdot S_{N,M}$.

7.2.3 MECC(N,M) loop shaping

Table 7.3 proposes a set of parameters for generalized MECC(N,M) loop shaping. Again, is has been attempted to minimize the degrees of freedom without compromising performance. The free parameters with the general parameter assignment in Table 7.3 are N, M and the bandwidths of the local global prototypes f_{uN} and f_{uM}. It should be emphasized that the MECC(N) should be optimized specifically towards the application of the global enhanced cascade. The local system should be optimized to provide best possible compensation, i.e. the bandwidth of the local system should be as high as possible. Reaching desired performance goals can carried by adjusting N and M. Only one local loop is necessary to provide the compensation. A feasible approach is to implement a MECC(1) system with sufficient compensation effect, and following adjust M to the

Parameter	Value	Comment
f_{uN}	≥ 8	MECC(N) parameter
$f_{i1} = \frac{1}{2\pi\tau_{i1}}$	f_o	MECC(N) parameter
f_{uM}	$\leq \frac{f_{uN}}{2}$	MECC(M,N) bandwidth defined
$f_1 = \frac{1}{2\pi\tau_1}$	f_o	Connection between local and global enhanced cascade.
$f_{i2} = \frac{1}{2\pi\tau_{i2}}$	$\frac{f_{uM}}{10}$	MECC(N,M) loop prototype parameter.
f_o	1	Demodulation filter natural frequency
Q_o	$\frac{1}{\sqrt{3}}$	Demodulation filter Q (Bessel)
f_r	3	Reference filter natural frequency
Q_r	$\frac{1}{\sqrt{3}}$	Reference filter Q (Bessel).

Table 7.3 Proposed MECC(N,M) parameter assignments.

desired performance. It should be emphasized, that the global enhanced cascade is independent upon *N*, since MECC(N) synthesizes a unique closed loop prototype as shown previously. The tradeoffs in MECC(N,M) design will become clearer throughout the more detailed investigation an illustrative case example.

7.2.4 MECC(N,M) case example

In the following, the characteristic of MECC(N,M) will be illustrated in detail with a case example.

STEP 1: Specification

The basic parameters are as for the MECC(N) case example. Performance requirements are only set for $\|S_{N,M}\|_\infty$, which should obey the general specifications in the nominal and perturbed case, as they were defined in Chapter 6. In terms of performance within the target band, a parametric analysis is carried out instead of designing towards a specific S_M specification. The prototype bandwidths of the specific case are set to:

$$f_{uN} = 10 \text{ and } f_{uM} = 4$$

These specifications obey the specified relationship in Table 7.3. *M* will be considered a variable parameter. *N* does not influence the global enhanced cascade and is set arbitrarily to 1.

STEP 2: Synthesis

With all fundamental parameters now determined, the MECC(N,M) controller synthesis is straightforward from the general parameter assignments in Table 7.3.

STEP 3: Verification

First consider the limiting case $f_{uN} \to \infty$. In this limiting case the global enhanced cascade realizes a higher order system with excellent stability, i.e.

$$\|S_{N,M}\|_\infty < 1 \quad \forall \omega, M \tag{7.38}$$

However, the bandwidth of the local MECC(N) system is inherently limited at $f_{uN} = 10$, and $S_{N,M}$ for the synthesized MECC(N,M) controller is shown in Fig. 7.16. The following is found by investigating $\|S_{N,M}\|_\infty$:

M	1	2	3	4
$\|S_{N,M}\|_\infty$	1.20	1.5	2.21	3.57

The system converges towards instability as the number of loops increase. *NS* is always guaranteed, however *NP* requires that $M \le 2$.

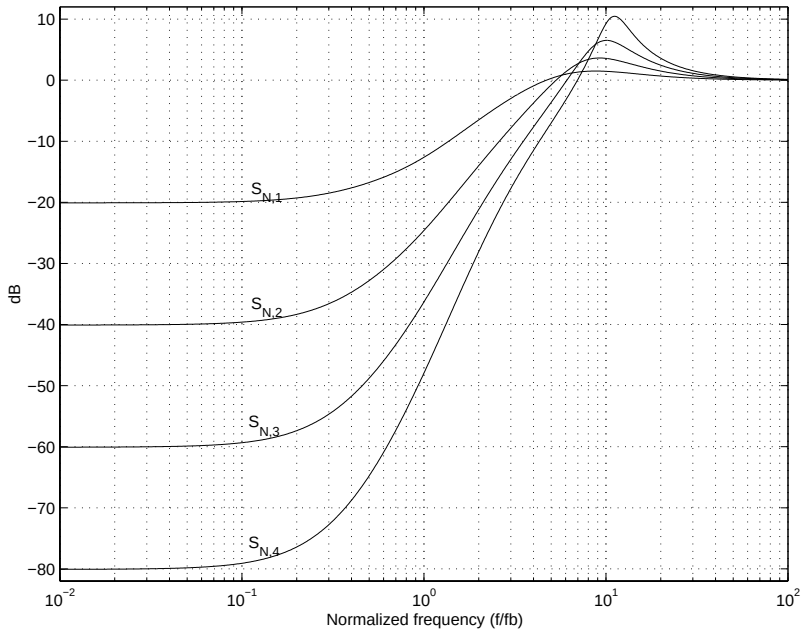

Fig. 7.16 $S_{N,M}$ for synthesized MECC(N,M) system $M = 1,2,3,4$.

Fig. 7.17 shows Bode-plots of all components of the MECC(N,M) system and Fig. 7.18 shows the system transfer function $H_{N,M}$ for $M = (1,2,3,4)$. Clearly, MECC(N,M) provides a much improved frequency response with the given parameters. Especially, the resulting response is excellent with both $M = 1$ and $M = 2$. The demodulation filter natural frequency is unity ($f_o = 1$), so the excellent frequency response characteristics do not compromise demodulation. The performance problems with $M \geq 2$ are also pronounced on the closed loop frequency response. Table 7.4 summarizes the essential results for the parametric results of the synthesized MECC(N,M) case example.

Specification	Value	Comments
System gain	*25.1 dB*	20dB feedback.
Bandwidth	2.5	Determined by R(s).
Frequency response	$\pm 0.01dB$	Nominal load. $M = 1$.
Frequency response	$\pm 0.3dB$	Nominal load. $M \leq 4$.
Phase response	$\pm 15^0$	Nominal load. $M \leq 4$
S_M	$-12 \cdot M\ dB$	Maximal effective sensitivity within bandwidth of interest

Table 7.4 Stability and performance specifications for the synthesized MECC (N,M) system.

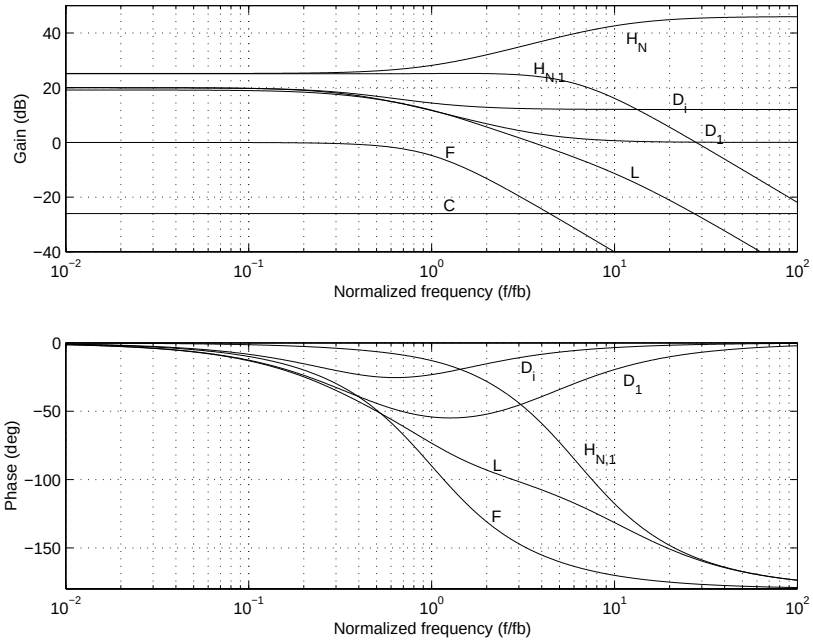

Fig. 7.17 Components of the MECC(N,M) system.

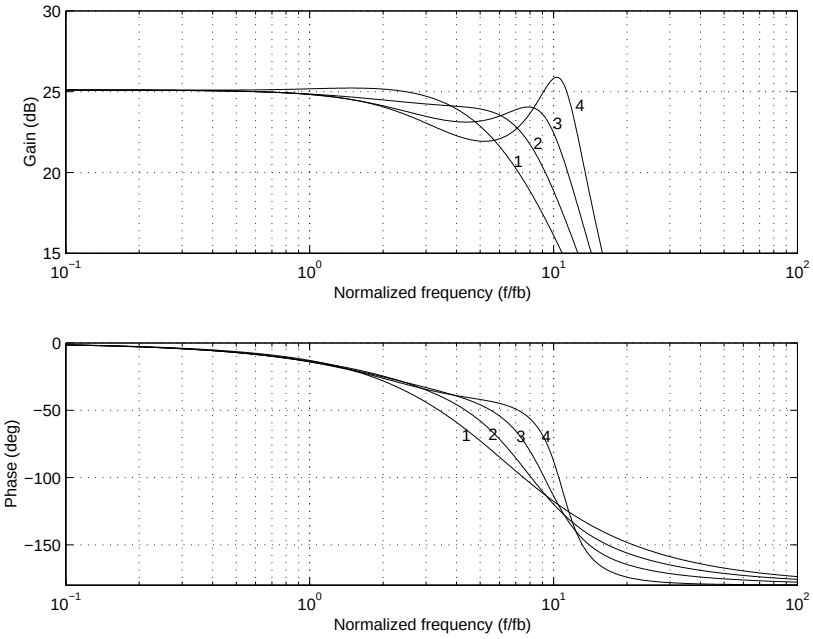

Fig. 7.18 Resulting system transfer function $H_{N,M}$, $M = 1,2,3,4$.

STEP4: MECC(N,M) Robustness properties

Recall from above, that MECC(N) proved very robust towards uncertainty on K_P and t_p. However, uncertainty on Q_0 will influence the MECC(N) frequency response notably, since the filter is not controlled. It is a more involved process to analyze the robustness properties for the general (N+M) loop MECC(N,M) topology. The perturbed loop transfer functions for the MECC(N,M) system can be written as:

$$L_{N,M,p}(r_K, r_Q, t_p) = H_{N,p}(r_K, r_Q, t_p) \cdot C \cdot F_p \sum_{j=0}^{M-1} \left[\prod_{i=1}^{M-j} D_i \right] \tag{7.39}$$

Where $H_{N,p}$ and F_p represents the perturbed version of the system response for MECC(N) and the demodulation filter, respectively. MECC(N,M) requires $f_{uM} << f_{uN}$ to implement the loop prototype in each loop. If this is not obeyed the stability and performance characteristics will be compromised, since the compensation provided by MECC(N) is only partial. Hence, it follows directly that MECC(N,M) is sensitive to uncertainty on K_P, since a reduced gain directly influences the *bandwidth* of the MECC(N) system. Fig. 7.19 shows a parametric investigation of the worst case perturbation within the Uncertainty Set, i.e. $S_{N,M,p}(0.5,4,200ns)$. The following peaks are found:

M	1	2	3	4
$\|S_{N,M,p}\|_\infty$	1.66	4.5	12.2	(unstab.)

Consequently, RS requires *M*<4 and RP requires *M*=1.

The effects of Q_o uncertainty are significantly different from MECC(N) since the filter is enclosed by the global enhanced cascade, with all the positive effects that follows. Fig. 7.20 shows the perturbed closed loop transfer function $H_{N,M,p}(1,4,0)$. Clearly, MECC(N,M) provides a much improved insensitivity to load variations. It can be concluded, that the system effectively suppresses the effects of filter uncertainty within the PMA bandwidth. The perturbed sensitivity function $S_{N,M,p}(1,4,0)$ corresponding to a worst-case perturbation on Q_o has the following maximal peaks:

M	1	2	3	4
$\|S_{N,M,p}\|_\infty$	1.29	1.81	2.83	5.40

RS always hold whereas RP requires *M<4*.

To conclude on the robustness investigations for MECC(N,M), the topology is specifically sensitive to large scale uncertainty on K_P due to the proportional relationship between the power stage gain and MECC(N) bandwidth. In the worst case-situation, only M=1 will satisfy both *RS* and *RP*. The robustness can be improved by a higher local bandwidth (f_{uN}) or alternatively a lower global bandwidth (f_{uM}). Perturbations on Q_o seen isolated are effective suppressed.

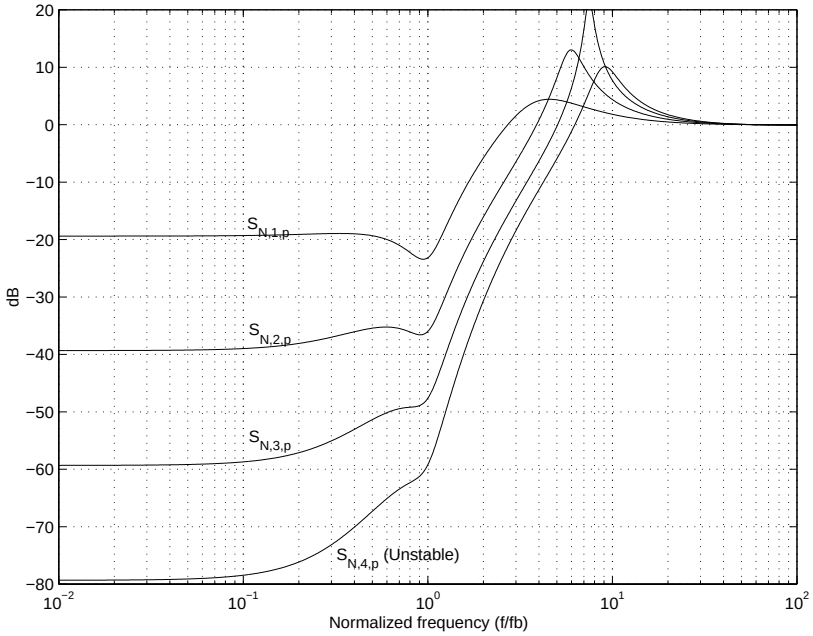

Fig. 7.19 Effective sensitivity function $S_{N,M,p}$ with ($M = 1,2,3,4$).

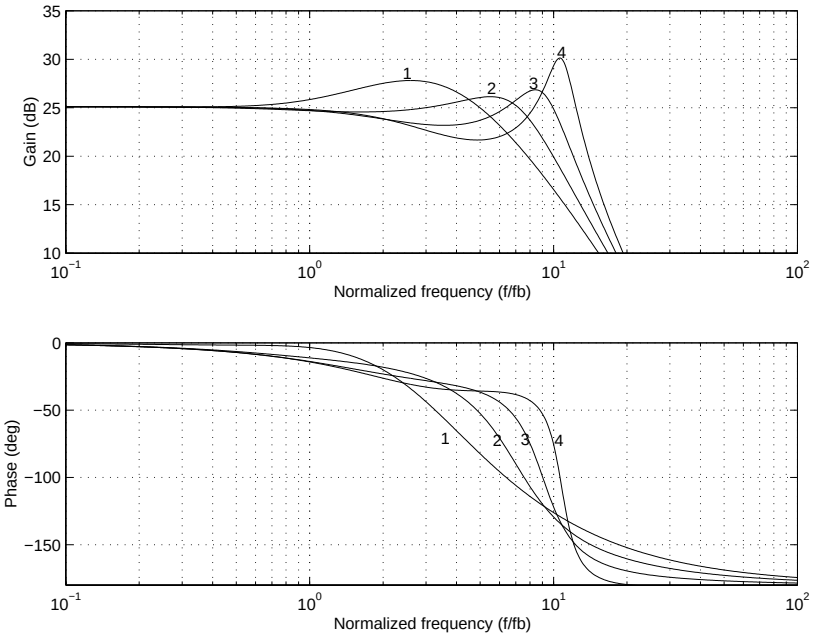

Fig. 7.20 System response $H_{N,M,p}$ with $r_Q = 4$ (worst-case). ($M = 1,2,3,4$).

STEP 5: MECC(N,M) - Nonlinear simulation

A triple loop case example (N,M)=(1,2) has been investigated on the non-linear PMA system, to investigate the properties for MECC(N,M) at low level. We derive for S_M :

$$S_M = S_1 \cdot S_{1,2} \approx -44dB$$

The parameters are as for the MECC(N) non-linear simulation and the local system has been implemented using the second order loop prototype to prevent Slew Rate Instability in the local feedback system. Fig. 7.21 shows a functional verification of the triple loop MECC(1,2) system. Note the pleasant signal levels on all compensator outputs (similar magnitude) – this is a general characteristic of both MECC(N) and MECC(N,M). It is also noted that the D_i compensator outputs are effective demodulated with a minimal amount of switching noise superposing the variables.

The MECC(1,2) topology has been subjected to the same tests in terms of correction effect towards different types of error sources, and the topology shows a correction capability that is comparable to the MECC(3) topology with the given parameters. This was to expect since the two systems have similar S_M , a since the fundamental concept of successive correction by the enhanced cascade has already been verified in the MECC(3) non-linear simulation.

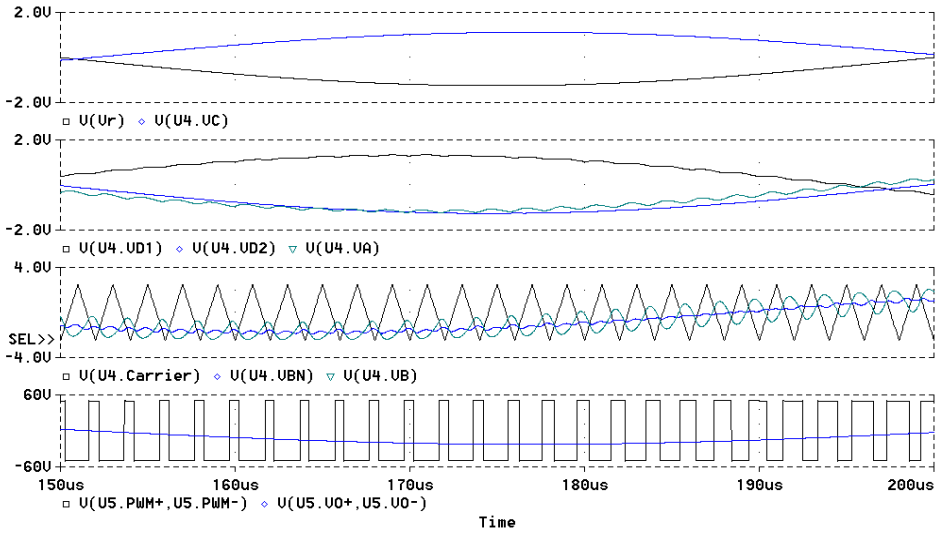

Fig. 7.21 Functional simulation of triple loop MECC(1,2) system. Top - Reference v_r and global feedback compensator (C) output v_c . Upper mid - Forward compensator (D_1, D_2) signals v_{d1} , v_{d2} and the local feedback compensator (A) output v_a . Lower mid – carrier and B_1 compensator output v_{b1} . Bottom – power stage output signals v_p and v_o .

7.3 Summary

The chapter has introduced an optimized control method – Multivariable Enhanced Cascade Control - that is dedicated to solve the problems within analog PMA systems. Two variants were introduced MECC(N) and MECC(N,M). Generally, MECC realizes a practical higher order system by an enhanced cascade structure, comprising a unique feedback path and a recursive structure of preferably identical forward paths compensators.

The concept of loop prototype based design was introduced to minimize the degrees of freedom within the higher order control structure. Loop prototypes were presented, and the general properties of MECC were investigated. General loop prototype based loop shaping was following addressed. The functionality of both MECC(N) and MECC(N,M) approaches has been verified by synthesizing and evaluating illustrative case examples.

Fundamentally, MECC offers a practical and robust method for higher order control system implementation with MECC(N) for dedicated applications and MECC(N,M) for general applications. MECC(N) has shown to provide several pleasant properties:

- Powerful and flexible control of the power stage is realized, with successive improvements for every loop added.
- Pleasing signal levels throughout the control structure. This provides immunity to e.g. switching noise from the power stage and other noise sources.
- Simplicity. The single feedback path minimizes complexity. Furthermore, the performance requirements of the individual compensator blocks are low.
- Excellent robustness to any perturbation within the *US*.
- Effective compensation of the demodulation filter, thus preparing the system for a global enhanced cascade.

MECC(N,M) encloses the PMA by two closely connected enhanced cascades. The additional properties of the MECC(N,M) are:

- Improved frequency response, insensitive to variable loading etc. Phase and amplitude response of the amplifier is much less dependent on the output filter.
- Error correction of filter errors, lowering the requirements for filter inductor linearity etc.

Although the chapter has been devoted to a generalized analysis, it should be emphasized that simple configurations as MECC(1,1), MECC(1,2) or MECC(1,2) can provide sufficient performance for even very non-linear and noisy plants. The pleasant combination of features combined with the simple realization, makes MECC the most powerful and flexible control method existing for general analog PMA systems.

7.3.1 MECCDIM – A GUI controlled toolbox for MATLAB

A GUI controlled MATLAB toolbox for systematic and automated design of MECC based PMAs has been developed. The graphical user interface is shown below.

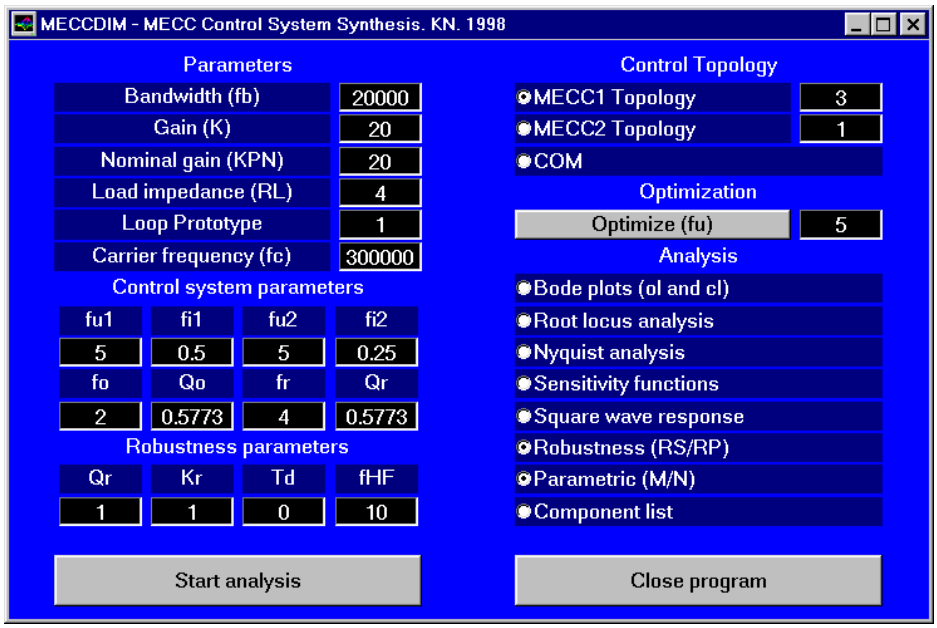

The toolbox provides automated design by simple push button access. Based on the primary amplifier input parameter specifications the interface gives access to:

- Optimal control system synthesis and verifications
- Parametric analysis (vs. M and N).
- Robustness investigations.
- Controller component synthesis for low-level non-linear simulation.
- Manual access to individual parameters for fine-tuning of performance to e.g. a specific application.

The program has been used extensively throughout the present chapter.